Am J Physiol Endocrinol Metab 296: E262–E271, 2009.
First published November 11, 2008; doi:10.1152/ajpendo.90678.2008.

Chronic infusion of angiotensin-(1–7) improves insulin resistance and hypertension induced by a high-fructose diet in rats

Jorge F. Giani,[1] Marcos A. Mayer,[2] Marina C. Muñoz,[1] Ezequiel A. Silberman,[2] Christian Höcht,[2] Carlos A. Taira,[2] Mariela M. Gironacci,[1] Daniel Turyn,[1] and Fernando Pablo Dominici[1]

[1]*Instituto de Química y Fisicoquímica Biológicas, Facultad de Farmacia y Bioquímica, and* [2]*Cátedra de Farmacología, Facultad de Farmacia y Bioquímica, Universidad de Buenos Aires, Buenos Aires, Argentina*

Submitted 5 August 2008; accepted in final form 8 November 2008

Giani JF, Mayer MA, Muñoz MC, Silberman EA, Höcht C, Taira CA, Gironacci MM, Turyn D, Dominici FP. Chronic infusion of angiotensin-(1–7) improves insulin resistance and hypertension induced by a high-fructose diet in rats. *Am J Physiol Endocrinol Metab* 296: E262–E271, 2009. First published November 11, 2008; doi:10.1152/ajpendo.90678.2008.—The current study was undertaken to determine whether Ang-(1–7) is effective in improving metabolic parameters in fructose-fed rats (FFR), a model of metabolic syndrome. Six-week-old male Sprague-Dawley rats were fed either normal rat chow (control) or the same diet plus 10% fructose in drinking water. For the last 2 wk of a 6-wk period of either diet, control and FFR were implanted with subcutaneous osmotic pumps that delivered Ang-(1–7) (100 $ng \cdot kg^{-1} \cdot min^{-1}$). A subgroup of each group of animals (control or FFR) underwent a sham surgery. We measured systolic blood pressure (SBP) together with plasma levels of insulin, triglycerides, and glucose. A glucose tolerance test (GTT) was performed, with plasma insulin levels determined before and 15 and 120 min after glucose administration. In addition, we evaluated insulin signaling through the IR/IRS-1/PI3K/Akt pathway as well as the phosphorylation levels of IRS-1 at inhibitory site Ser^{307} in skeletal muscle and adipose tissue. FFR displayed hypertriglyceridemia, hyperinsulinemia, increased SBP, and an exaggerated release of insulin during a GTT, together with decreased activation of insulin signaling through the IR/IRS-1/PI3K/Akt pathway in skeletal muscle, liver, and adipose tissue, as well as increased levels of IRS-1 phospho-Ser^{307} in skeletal muscle and adipose tissue, alterations that correlated with increased activation of the kinases mTOR and JNK. Chronic Ang-(1–7) treatment resulted in normalization of all alterations. These results show that Ang-(1–7) ameliorates insulin resistance in a model of metabolic syndrome via a mechanism that could involve the modulation of insulin signaling.

serine phosphorylation; renin-angiotensin system; insulin signaling

INSULIN RESISTANCE PLAYS A FUNDAMENTAL ROLE in the development of the metabolic syndrome, defined as a group of abnormalities including impaired glucose tolerance, hypertension, and dyslipidemia (10, 12, 20, 46). Although this area is focus of intense clinical and basic research, the molecular mechanisms linking insulin resistance to hypertension are not well understood (37).

Alterations within the renin-angiotensin (Ang) system (RAS) are important contributors to the development of insulin resistance (22, 37, 44). The current view representing the functional outline of the RAS is composed of two arms. The first arm is represented by Ang II and is characterized by hypertensive and hypertrophic effects originating from an enzymatic cascade in which angiotensinogen is converted to Ang I and then to Ang II by the actions of renin and angiotensin-converting enzyme (ACE), respectively (14, 22, 42). The second arm is antihypertensive and antihypertrophic of nature, where the major participant is Ang-(1–7), a heptapeptide that constitutes an important functional end product of the RAS and is formed primarily from Ang II and Ang I by ACE 2 (14, 22, 42).

Ang II plays a critical role in the etiology of insulin resistance (38, 39). The mechanism behind this deleterious effect appears to be related to a negative modulation exerted by Ang II on several steps of the insulin-signaling cascade, including insulin-induced phosphorylation of the insulin receptor (IR) insulin receptor substrate-1 (IRS-1) and activation of Akt by phosphatidylinositol 3-kinase (PI3K) (47). Accordingly, clinical trials have shown that inhibition of ACE or selective Ang type 1 receptor blockade reduces the development of type 2 diabetes in patients with essential hypertension (3, 27). In line with reports in humans, improvement of insulin sensitivity (15, 21, 22, 23, 45), along with an enhancement in the response to insulin at various steps of the insulin-signaling cascade (8, 33, 34), has been detected in various animal models of insulin resistance and/or type 2 diabetes as a consequence of reduction of Ang II formation or inhibition of its actions. This evidence clearly indicates that the signaling cross-talk between insulin and Ang II has significant physiological relevance.

Ang-(1–7), through its specific G protein-coupled receptor Mas, induces responses opposing those of Ang II, including antihypertensive, antihypertrophhic, antifibrotic, and antithrombotic properties (14, 26, 42). In a previous work, we demonstrated that Ang-(1–7) is able to modulate the insulin-signaling pathway by inducing Akt phosphorylation via the Mas receptor (17). In addition, it was shown that Ang-(1–7) overcomes the inhibition of insulin-induced phosphorylation of Akt phosphorylation by Ang II (17). The action of Ang-(1–7) on insulin pathways indicated a role in metabolic processes. Recently, Santos et al. (43) reported that genetic deletion of Mas receptor leads to a metabolic syndrome state in mice. These findings are in keeping with our results and support a putative new physiological function of Ang-(1–7) in glycemic control and insulin resistance. The current study was undertaken to determine whether Ang-(1–7) is effective in improving metabolic parameters in fructose-fed rats, a model of insulin resistance with dyslipidemia and mild hypertension. We provide physiological and molecular evidence for Ang-(1–

Address for reprint requests and other correspondence: F. P. Dominici, IQUIFIB, Facultad de Farmacia y Bioquímica, Universidad de Buenos Aires, Junín 956, (1113), Buenos Aires, Argentina (e-mail: dominici@qb.ffyb.uba.ar).

The costs of publication of this article were defrayed in part by the payment of page charges. The article must therefore be hereby marked "*advertisement*" in accordance with 18 U.S.C. Section 1734 solely to indicate this fact.

7)-induced improvement in metabolic and hemodynamic parameters [insulin sensitivity, triglyceridemia, and systolic blood pressure (SBP)] and provide new insights into possible insulin sensitization mechanisms of Ang-(1–7).

MATERIALS AND METHODS

Materials. The peptide Ang-(1–7) was synthesized in our laboratory as described previously (14). The reagents and apparatus for SDS-PAGE and immunoblotting were obtained from Bio-Rad (Hercules, CA). The monoclonal anti-phosphotyrosine antibody (anti-PY; PY99), the polyclonal anti-IR β-subunit antibody (anti-IR; C-19), the polyclonal anti-phospho-c-Jun NH_2-terminal kinase (JNK) mouse monoclonal antibody (sc-6254), the goat polyclonal antibody that detects the inhibitor of κB kinase (IKKβ) when phosphorylated at Ser^{181} (sc-23470), goat anti-rabbit IgG conjugated with horseradish peroxidase (HRP), and goat anti-mouse IgG-HRP secondary antibodies were purchased from Santa Cruz Biotechnology (Santa Cruz, CA). The polyclonal antiserum against the p85 subunit of PI3K (anti-p85; 06-195) was purchased from Upstate Biotechnology (Lake Placid, NY). The polyclonal anti IRS-1 antibody (anti-IRS-1; 2382), the phospho-Akt (Thr^{308}) rabbit monoclonal antibody that detects endogenous levels of Akt only when phosphorylated at Thr^{308} (9275), the polyclonal Akt antibody that detects endogenous levels of total Akt1, Akt2, and Akt3 proteins (anti-Akt; 9272), the phospho-IRS-1 Ser^{307} polyclonal antibody (2381), the rabbit polyclonal antibodies against the kinase mammalian target of rapamycin (mTOR; 2972) and phospho-mTOR (Ser^{2448}; 2971), the rabbit monoclonal antibody anti-JNK (9528), and the IKKβ rabbit polyclonal antibody (2684) were purchased from Cell Signaling (Beverly, MA). Enhanced chemiluminescence (ECL) was from Amersham (Piscataway, NJ). The remaining reagents were purchased from Sigma Chemical (St. Louis, MO).

Animals and treatments. A total of 48 male Sprague-Dawley rats weighing 220–240 g were used for this study. All animals were housed individually in a controlled environment with a photoperiod of 12:12-h light-dark (lights on from 0600 to 1800) and a temperature of 20 ± 2°C. Housing, handling, and experimental procedures followed the rules written in the *Guide for the Care and Use of Laboratory Animals* published by the National Institutes of Health [DHEW Publication No. (NIH) 85-23, revised 1996, Office of Science and Health Reports, Division of Research Resources/NIH, Bethesda, MD 20205] and were approved by the Laboratory Animal Use and Care Committee of the School of Pharmacy and Biochemistry of the University of Buenos Aires. Following an acclimatization period of 7 days, rats were randomly divided into two groups, a control group ($n = 24$) that received regular diet (19% protein, 77% carbohydrate, 4% fat) and a fructose-fed group ($n = 24$) that was fed a regular diet and fructose that was administered as a 10% solution (prepared every 2 days) in drinking water for 6 wk, as described previously (32). Control animals were given ordinary tap water to drink throughout the entire experimental period. Animals consumed diets and fluids ad libitum. For the last 2 wk of either feeding period, 12 animals from the control group and 12 from the fructose-fed group were implanted with subcutaneous osmotic pumps (model 2002; Alzet) that delivered Ang-(1–7) (100 $ng \cdot kg^{-1} \cdot min^{-1}$). The rest of the animals (12 in each group) underwent a sham surgery.

SBP and body weight determination. Rats were weighed previously to dietary manipulation and at the end of the study. The rats were trained to the procedure of SBP measurement at 1300 twice/wk for 2 wk previous to the final measurement. The mean of 10 consecutive readings was used as the reported value of the SBP for each rat. Indirect SBP was measured at *week 4* and *week 6* by means of the tail-cuff method using a blood pressure analysis system (model SC1000; Hatteras Instruments).

Glucose, triglycerides, and insulin measurements. All corresponding measurements were determined 6 h after food removal. Blood glucose measurements were performed using a hand-held glucometer (Accucheck, Mannheim, Germany). Insulin levels were assessed using a rat insulin ELISA kit (Ultra Sensitive Rat Insulin ELISA Kit; Crystal Chem). Circulating triglyceride (TG) concentrations were measured by an enzymatic colorimetric assay kit (Wiener Lab, Rosario, Argentina).

The homeostasis model assessment of basal insulin resistance (HOMA-IR) was used to calculate an index from the product of the fasting concentrations of plasma glucose (mmol/l) and plasma insulin (μU/ml) divided by 22.5 (31). Lower HOMA-IR values indicated greater insulin sensitivity, whereas higher HOMA-IR values indicated lower insulin sensitivity (insulin resistance).

Glucose tolerance test. After a 6-h fast the rats were anesthetized, and after the collection of an unchallenged sample (*time 0*), a solution of 50% glucose (2.0 g/kg body wt) was administered into the peritoneal cavity. During the test, blood was collected from the tail vein 15, 30, 60, 90, and 120 min after glucose administration. All blood glucose measurements were performed using a hand-held glucometer. Serum insulin levels were measured at baseline and 15 and 120 min postglucose administration by ELISA, as described above.

Acute insulin stimulation and tissue collection. After the 2-wk treatment with Ang-(1–7), rats were starved overnight, anesthetized by the intraperitoneal administration of a mixture of ketamine and xylazine (50 and 1 mg/kg, respectively), and submitted to the surgical procedure as soon as anesthesia was assured by the loss of pedal and corneal reflexes. The abdominal cavity was opened, the portal vein was exposed, and 10 IU porcine insulin/kg body wt in normal saline (0.9% NaCl) in a final volume of 0.2 ml was injected via this vein. To obtain data under basal conditions, rats received an injection of diluent. The liver, adipose tissue (epididymal), and skeletal muscle (soleus) were removed after 1, 3, and 5 min, respectively, and kept at −80°C until analysis.

Tissue homogenization, immunoprecipitation, Western blotting analysis, and quantification of phosphorylation of IRS-1 at Ser^{307} by ELISA. Tissue samples were homogenized in solubilization buffer containing 1% Triton together with phosphatase and protease inhibitors, as described previously (17, 33). Tissue extracts were centrifuged at 100,000 *g* for 1 h at 4°C to eliminate insoluble material, and protein concentration in the supernatants was measured using the Bradford method, as described previously (17, 33). Equal amounts of solubilized protein (2 mg) were incubated at 4°C overnight with anti-IR or anti-IRS-1 antibodies at a final concentration of 4 μg/ml. Immune complexes were collected by incubation with protein A-Sepharose 6 MB, as described previously (17, 33). SDS-PAGE and Western transfer of proteins to PVDF membranes were performed as described previously (17, 33). Membranes were blocked by incubation for 2 h with Tris-buffered saline containing 0.1% Tween-20 and 3% BSA and subsequently incubated overnight with the anti-phosphotyrosine antibody (1:1,000) to detect tyrosine phosphorylation. Membranes were reblotted with anti-IR (1:200) or anti-IRS-1 (1:1,000) to determine protein abundance of these two proteins. To determine the amount of the p85 subunit of PI3K associated with IRS-1, membranes corresponding to anti-IRS-1 immunoprecipitates were also reprobed with anti-p85 antibody (1:2,000). To determine the phosphorylation of IRS-1 at Ser^{307}, IRS-1 immunoprecipitates were probed with the anti-phospho-IRS-1 (Ser^{307}) antibody (1:1,000). To determine the phosphorylation levels of Akt, JNK, mTOR, or IKK, equal amounts of solubilized proteins (40 μg) were denatured by boiling in reducing sample buffer, resolved by SDS-PAGE, and subjected to immunoblotting with the corresponding phospho-specific antibodies (1:1,000 dilution). Protein abundance was detected by reprobing membranes with the corresponding antibodies. After extensive washing, membranes were incubated with the appropriate secondary HRP-coupled antibodies and processed for ECL using the ECL plus Western Blotting detection system (Amersham Biosciences). Bands were quantified using Gel-Pro Analyzer 4.0 (Media Cybernetics, Bethesda, MD). IRS-1 phospho-Ser^{307} levels were measured in aliquots of homogenates containing 0.2 mg of protein using a commercial solid-

phase sandwich ELISA (catalog no. KH00521; Biosource, Camarillo, CA) in accordance with the manufacturer's instructions.

Statistical analysis. All values are reported as means ± SE unless specified otherwise. The statistical significance of differences in mean values between the four animal groups was assessed by two-way ANOVA. A value of $P < 0.05$ was considered statistically significant.

RESULTS

Metabolic characteristics of the experimental animals and effect of Ang-(1–7) treatment. At the end of 6-wk high-fructose diet feeding, body weights were similar between standard chow-fed and fructose-fed rats (Table 1). As expected, on the basis of published data in the fructose-fed rat model (9, 32, 41), circulating insulin and TG were significantly higher in the group consuming high-fructose diet than in the standard chow-fed group (Table 1). In addition, fructose-fed rats developed a mild hypertensive state, as shown by a significant increase in SBP ($P < 0.05$ vs. control rats). Glucose levels remained unaltered after fructose overload (Table 1). Remarkably, circulating insulin and TG levels in fructose-fed rats that were chronically treated for 14 days with Ang-(1–7) fell to a value significantly lower than the sham counterparts ($P < 0.05$). Also, Ang-(1–7) caused a significant decrease in SBP in fructose-fed rats (88% of mean fructose-fed values, $P < 0.05$). Consequently, metabolic parameters and SBP in fructose-fed rats that were chronically treated with Ang-(1–7) rats were not statistically different from those displayed by the control group at the end of the study (Table 1). In control animals, treatment with Ang-(1–7) did not significantly alter circulating glucose, TG, insulin, or SBP (Table 1). Additionally, the HOMA score in fructose-fed rats was higher by 2.8-fold times that of the control group. Following 14 days of Ang-(1–7) treatment, the HOMA score in fructose-fed rats markedly fell to 49% of that in their sham-implanted counterparts (Table 1). Furthermore, we found that the HOMA score of control rats was not altered after treatment with Ang-(1–7) (Table 1).

Ang-(1–7) improves insulin sensitivity in fructose-fed rats. The response to an intraperitoneal glucose tolerance test (IPGTT) at the termination of 2-wk treatment with Ang-(1–7) is shown in Fig. 1. Plasma glucose levels increased significantly during the IPGTT in all groups of animals. Compared with the control sham group, the fructose sham group of rats presented a tendency to an increase in the glucose area under the curve during the IPGTT (Fig. 1). However, this change did not reach statistical significance ($P = 0.1$). Treatment with Ang-(1–7) did not exert a significant influence on glucose tolerance in either control or fructose-fed rats (Fig. 1). Fasting plasma insulin concentrations were measured at baseline and 15 and 120 min after glucose injection. Circulating insulin concentrations were significantly larger in fructose-fed rats compared with the control group at baseline (2.4-fold increase, $P < 0.05$) 15 min after injection (2.2-fold increase, $P < 0.05$) and remained significantly higher after 120 min (2.1-fold increase, $P < 0.05$). This altered insulin secretory response would suggest a state of insulin resistance in the fructose-fed rats. The insulin secretory response was sensibly reduced in fructose-fed rats after Ang-(1–7) treatment compared with their sham counterparts, indicative of an amelioration of the insulin-resistant state after chronic treatment with Ang-(1–7). This

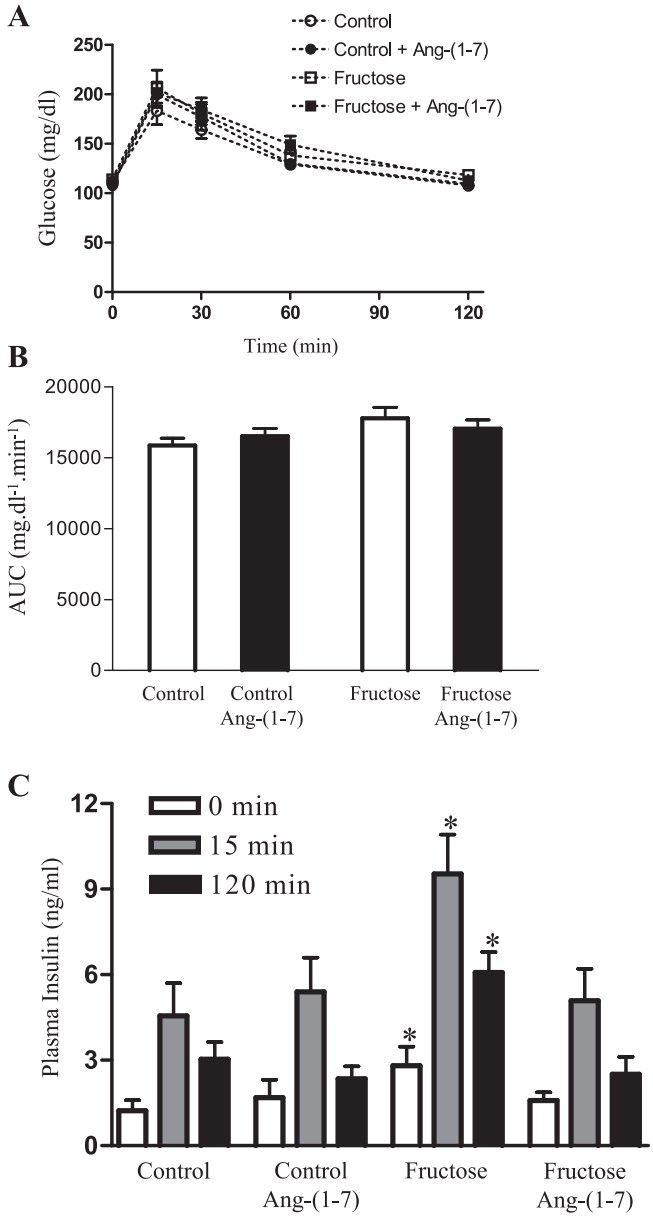

Fig. 1. Glycemic profile. *A*: glucose tolerance test. Rats were fasted for 6 h and given an intraperitoneal injection of glucose (2 mg/g body wt). Data are presented as mean of plasma glucose levels (mg/dl) ± SE from 6 rats in each group. *B*: area under the glucose tolerance test curves (AUC). *C*: serum insulin concentrations; serum insulin levels attained during the glucose tolerance test. *$P < 0.05$ vs. the corresponding values in all other groups. Ang-(1–7), angiotensin-(1–7).

Table 1. *Metabolic parameters of the experimental animals*

Parameters	Control		Fructose	
	Sham	Ang-(1–7)	Sham	Ang-(1–7)
Body weight, g	380±9	362±9	385±12	375±7
SBP, mmHg	112±14	116±4	135±7*	120±4
Fasted glycemia, mg/dl	112±9	109±9	114±10	112±11
Plasma insulin, ng/ml	1.2±0.2	1.6±0.2	2.8±0.4*	1.6±0.3
Triglycerides, mg/dl	82±13	71±11	176±18*	115±12
HOMA score	2.8±0.9	3.1±0.9	7.9±1.7*	3.9±0.7

Values are means ± SE ($n = 12$ animals in each group). Ang-(1–7), angiotensin-(1–7); SBP, systolic blood pressure; HOMA, homeostasis model assessment. *Value significantly different from control sham value ($P < 0.05$).

result is in line with the observation of reduced circulating TG and insulin after infusion with Ang-(1–7). Treatment with Ang-(1–7) for 14 days did not significantly modify the release of insulin during the IPGTT in the sham-implanted animals fed a regular diet (Fig. 1).

Angiotensin-(1–7) improves insulin signal transduction in skeletal muscle, adipose tissue, and liver. Fructose feeding is known to produce an impairment of insulin signaling in rats (6, 30). In this study we evaluated insulin signaling through the IR/IRS-1/PI3K/Akt pathway in insulin target tissues of rats fed on regular chow or with fructose in drinking water. An impairment in all steps of insulin signaling analyzed IR (Fig. 2), IRS-1 (Fig. 3), and p85-IRS-1 association (Fig. 4), and Akt phosphorylation (Fig. 5) was detected in skeletal muscle, adipose tissue, and liver of fructose-fed rats. To determine the effect of chronic Ang-(1–7) on insulin signal transduction, Sprague-Dawley rats fed with 10% fructose on drinking water were treated with Ang-(1–7) for 14 days and evaluated for insulin signaling in the tissues described above. As shown in Figs. 2–5, significant improvement in insulin signal transduction through the steps that result in activation of Akt was detected in skeletal muscle, adipose tissue, and liver of rats treated with Ang-(1–7). As detected by specific immunoblotting, changes in phosphorylation were not the consequence of changes in the abundance of the signaling proteins analyzed (Figs. 2–5).

Treatment of fructose-fed rats with Ang-(1–7) is associated with decreased phosphorylation of IRS-1 on Ser^{307} and decreased activation of the kinases JNK and mTOR in skeletal muscle and white adipose tissue. To address the mechanism involved in the improvement of insulin signaling and action in fructose-fed rats originated by treatment with Ang-(1–7), we measured the levels of IRS-1 phosphorylation at the inhibitory residue Ser^{307} in peripheral insulin target tissues muscle and white adipose tissue. As shown in Fig. 6, compared with values found in control rats, there was a significant increase in IRS-1 Ser^{307} phosphorylation in rats fed with fructose in both skeletal muscle (35% as measured by ELISA and 120% as measured by immunoblotting, $P < 0.05$ in both cases) and white adipose tissue (22% as measured by ELISA and 126% as measured by immunoblotting, $P < 0.05$ in both cases). Treatment of fructose-fed rats with Ang-(1–7) was found to reduce IRS-1 Ser^{307} phosphorylation to control values in both tissues, whereas it did not induce significant changes in control animals (Fig. 6). This modulation of phospho-IRS-1 Ser^{307} was independent of modulation of total IRS-1 levels (Fig. 6).

To further evaluate this mechanism of inhibition of the insulin-signaling pathway in fructose-fed rats as well as the impact of Ang-(1–7) treatment, we evaluated the phosphorylation status of JNK, mTOR, and IKKβ, three kinases involved in the signaling pathway responsible for the phosphorylation of IRS-1 upon Ser^{307}. As shown in Fig. 7, fructose-fed rats showed a significant increase in the phosphorylation levels of JNK and mTOR in skeletal muscle (increases of 94 and 202%, respectively, $P < 0.05$ vs. control rats) and adipose tissue (increases of 47 and 203%, respectively, $P < 0.05$ vs. control rats). In contrast, the phosphorylation levels of IKKβ remained unaltered after fructose treatment.

The protein abundance of the kinases analyzed was unaltered by the fructose treatment (Fig. 7, *bottom*).

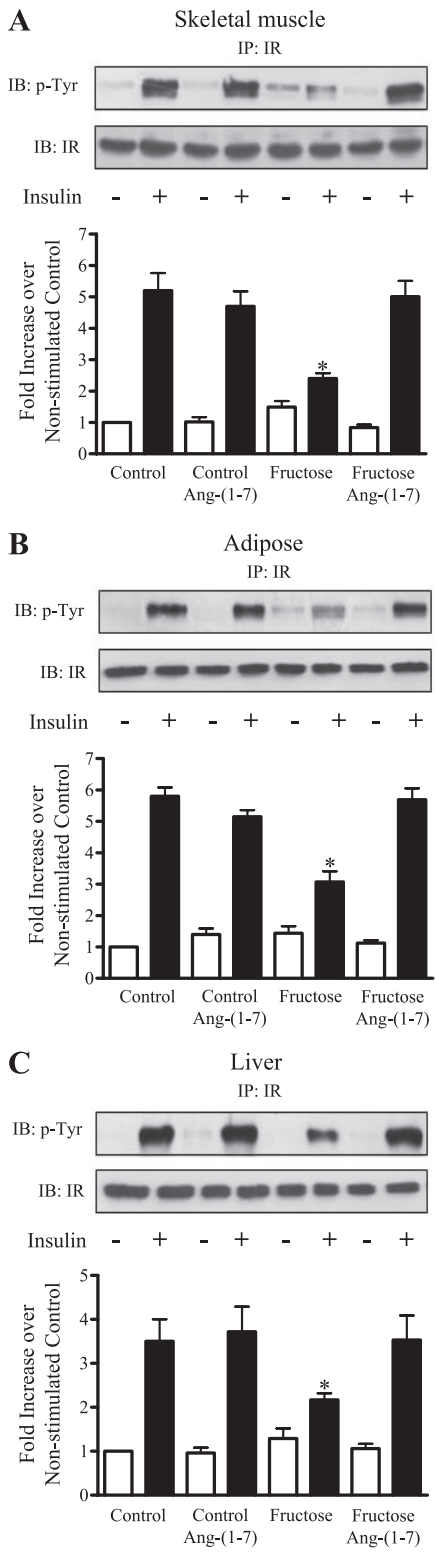

Fig. 2. Tyrosine phosphorylation (p-Tyr) of the insulin receptor (IR) in vivo. Rats were injected via portal vein with porcine insulin. The skeletal muscle (*A*), adipose tissue (epididymal; *B*), and liver (*C*) were removed 5, 3, and 1 min, respectively, after injection, and tyrosine phosphorylation was measured by specific immunoblotting (IB) in IR immunoprecipitates (IP). To determine receptor abundance, membranes were reprobed with an anti-IR antibody. Quantification of phosphorylation by scanning densitometry is given below immunoblots. Scanning data obtained from 6 independent experiments are expressed as fold increase over saline-injected (basal) control phosphorylation ± SE. *$P < 0.05$ vs. insulin-stimulated control values.

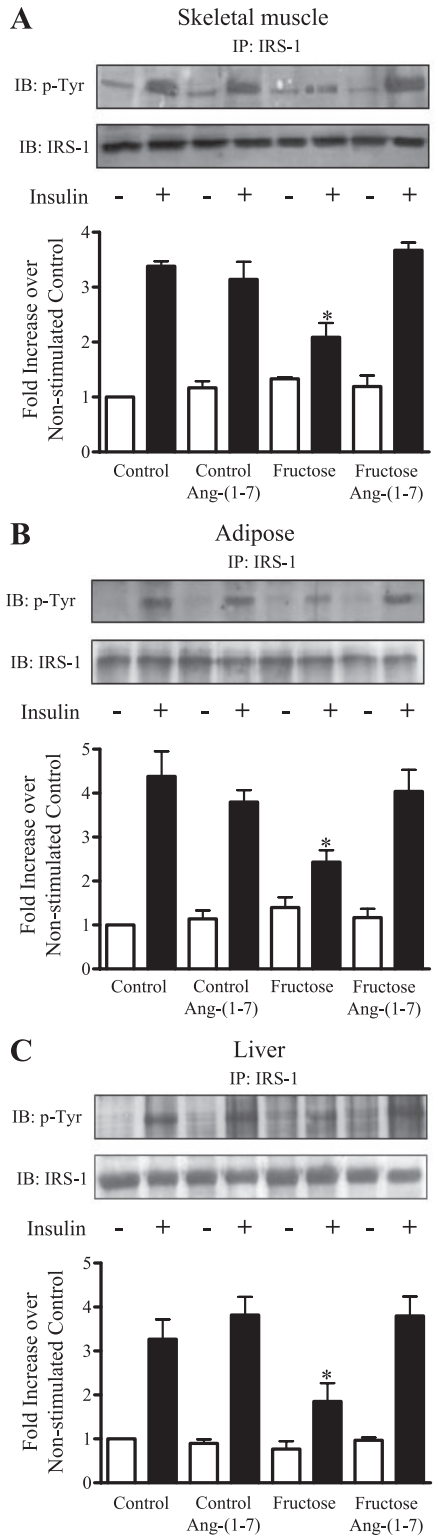

Fig. 3. p-Tyr of insulin receptor substrate (IRS-1). Rats were injected via portal vein with porcine insulin. The skeletal muscle (*A*), adipose tissue (epididymal; *B*), and liver (*C*) were removed 5, 3, and 1 min, respectively, after injection, and p-Tyr was measured by specific IB in IRS-1 IP. To determine IRS-1 abundance, membranes were reprobed with an anti-IRS-1 antibody. Quantification of phosphorylation by scanning densitometry is given below IB. Scanning data obtained from 6 independent experiments are expressed as fold increase over saline-injected (basal) control phosphorylation ± SE. *$P < 0.05$ vs. insulin-stimulated control values.

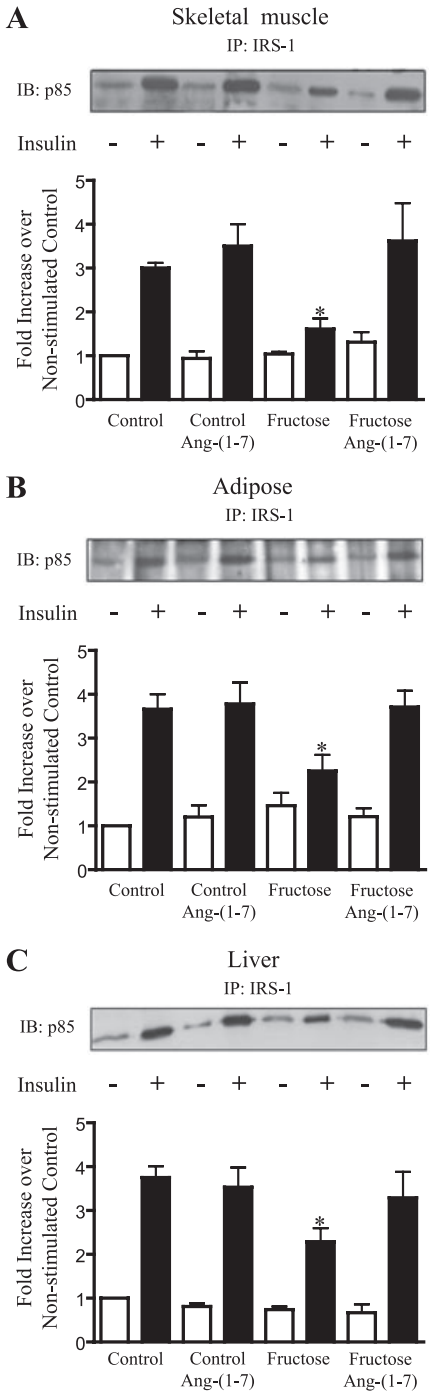

Fig. 4. Association between the p85 regulatory subunit of phosphatidylinositol 3-kinase (PI3K) and IRS-1. Rats were injected via portal vein with porcine insulin. The skeletal muscle (*A*), adipose tissue (epididymal; *B*), and liver (*C*) were removed 5, 3, and 1 min, respectively, after injection, and the amount of p85 was measured by specific immunoblotting in IRS-1 IP. Quantification of p85 associated with IRS-1 by scanning densitometry is given below IB. Scanning data obtained from 6 independent experiments are expressed as fold increase over saline-injected (basal) control p85-IRS-1 association ± SE. *$P < 0.05$ vs. insulin-stimulated control values.

DISCUSSION

The major finding of this study was that chronic Ang-(1–7) treatment resulted in a reversal of fructose-induced insulin resistance. The favorable effects of chronic Ang-(1–7) treat-

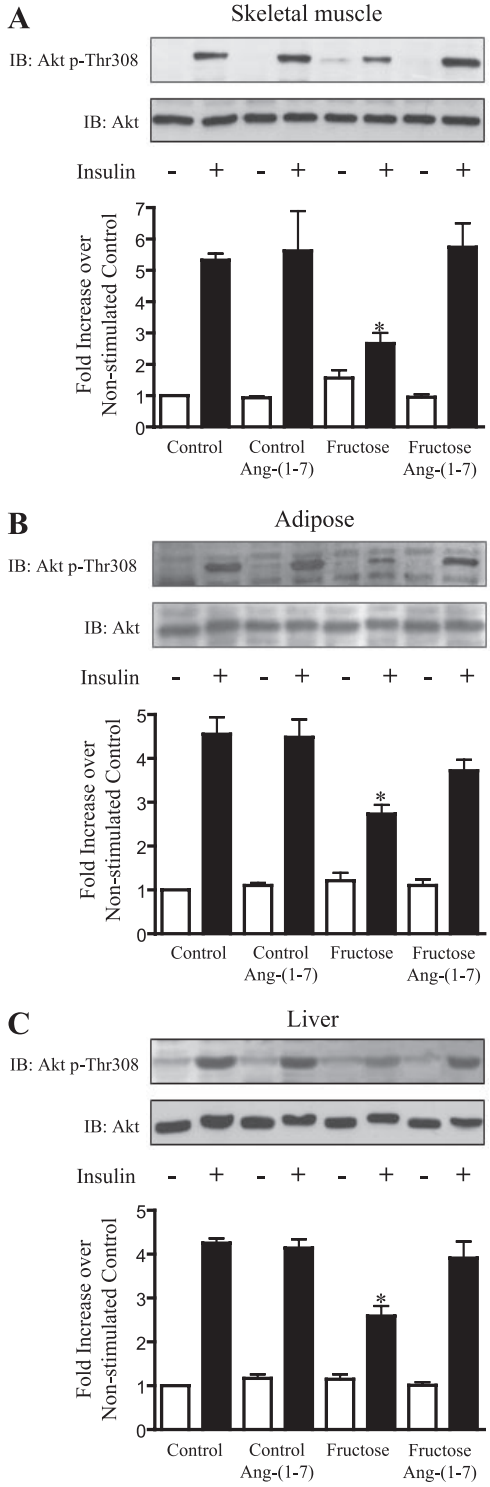

Fig. 5. Phosphorylation of Akt on Thr^{308} (p-Thr^{308}). Rats were injected via portal vein with porcine insulin. The skeletal muscle (*A*), adipose tissue (epididymal; *B*), and liver (*C*) were removed 5, 3, and 1 min, respectively, after injection, and p-Thr^{308} was measured by specific IB. Membranes were re-probed with an anti-Akt antibody to determine Akt abundance. Quantification of phosphorylation by scanning densitometry is given below immunoblots. Scanning data obtained from 6 independent experiments are expressed as fold increase over saline-injected (basal) control phosphorylation ± SE. *$P < 0.05$ vs. insulin-stimulated control values.

ment in insulin-resistant animals included reduction of fasting triglyceride and insulin levels, reduction of systolic blood pressure, and restoration of insulin signaling through the IR/IRS-1/PI3K/Akt pathway in the main target tissues of insulin: skeletal muscle, liver, and adipose tissue. Together with recent demonstration that genetic deletion of Mas in FVB/N mice leads to a metabolic syndrome-like state (43), our present findings indicate that the Mas/Ang-(1–7) axis could participate in glycemic control.

The RAS is known to play an important role in insulin resistance and diabetes, Ang II being an important mediator of adverse processes (38, 39). On the other hand, Ang-(1–7) appears to exert a protective role in diabetes. Recent reports indicate that Ang-(1–7) attenuates proteinuria, protects the heart in response to ischemia/reperfusion, and restores the normal function of the renal vasculature in diabetic rats (4, 5). We have shown that Ang-(1–7) modulates the insulin-signaling pathway (17), suggesting that this beneficial effect of Ang-(1–7) could be the result of such modulation. This putative new physiological function of Ang-(1–7) was the subject of exploration of the current study.

The fructose-fed rat model is a commonly used environmentally induced model that mimics human metabolic syndrome in many aspects, including hypertension, hypertriglyceridemia, insulin resistance, and compensatory hyperinsulinemia. Fructose-induced metabolic syndrome can be created experimentally by either adding fructose to drinking water (10–20%) (9, 32, 41) or feeding rats with a high-fructose diet (60%) (6, 30). In the present study, we looked at Ang-(1–7) on insulin resistance induced by administration of 10% fructose in drinking water, which proved to induce a prediabetic state, as shown by the need for augmented insulin release to maintain euglycemia in the face of a glucose challenge. Previous studies have shown that circulating Ang II levels are increased in fructose-fed rats (29). In addition, administration of both Ang II receptor antagonists (15, 25, 28, 36) or ACE inhibitors (13, 23) has been shown to revert the insulin resistance in fructose-fed rats, strongly suggesting that Ang II is involved in the insulin-resistant state developed by fructose overload. In view of these data, and given that Ang-(1–7) counteracts most of Ang II actions, we hypothesize that, in part, our current observation showing reversal of insulin resistance in fructose-fed rats after Ang-(1–7) treatment could be the result of a counterbalance exerted by Ang-(1–7) on the deleterious effects of Ang II with regard to lipid and carbohydrate metabolism.

It is worth mentioning that chronic treatment with Ang-(1–7) using the same dose and methodology employed in the current study has previously proven to have a therapeutic effect. Grobe et al. (18) demonstrated that delivery of Ang-(1–7) prevents Ang II-induced cardiac remodeling. In addition, these authors demonstrated that chronic treatment with Ang-(1–7) prevents cardiac fibrosis in rats treated with deoxycorticosterone acetate (19).

The mechanism behind the amelioration of insulin resistance and improvement of insulin signaling induced by Ang-(1–7) in fructose-fed rats is intriguing and deserves further exploration. One potential mechanism involved could be the ability of Ang-(1–7) to activate, unlike Ang II, the enzyme Akt, a phenomenon that has been described in both endothelial cells and in the heart and is associated with Mas receptor activation (17, 40). It is important to consider that, at least in the heart,

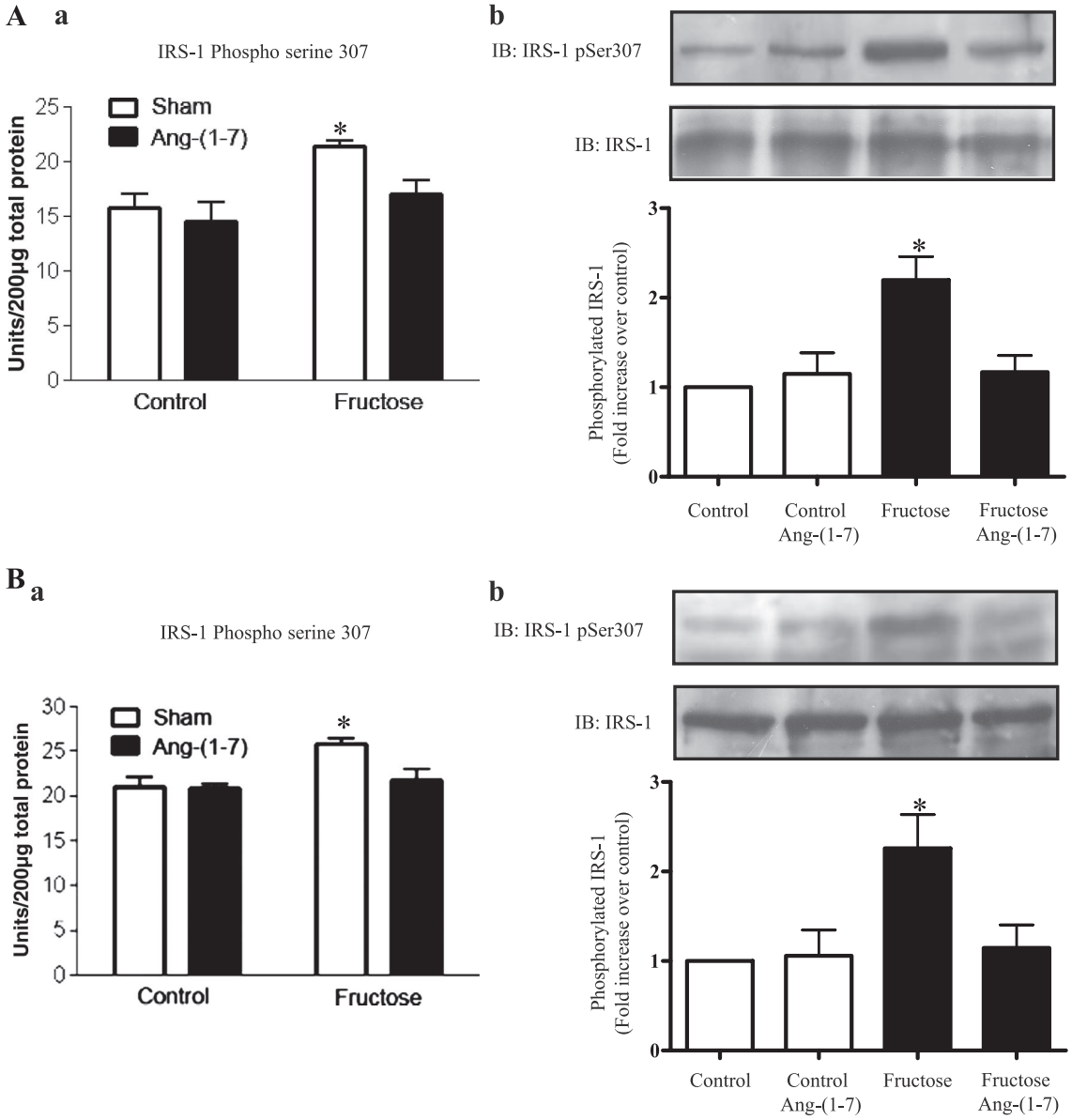

Fig. 6. Phosphorylation of IRS-1 on Ser^{307}. Data are from saline-injected rats, as described in the legend to Fig. 1. Phospho (p)-Ser^{307} levels were measured in tissue homogenates (*A*: skeletal muscle; *B*: adipose tissue) by the use of a specific ELISA (*a*) or by means of IP of tissue proteins with an anti-IRS-1 antibody followed by IB with an anti-phospho-IRS-1 (Ser^{307}) antibody (*b*). To determine protein abundance, membranes were reprobed with the anti-IRS-1 antibody. Data are means ± SE ($n = 6$). *$P < 0.05$ vs. all other groups.

Ang-(1–7) antagonizes the inhibitory effects of Ang II on insulin-induced activation of Akt (17). Thus, the observed improvement in insulin signaling after Ang-(1–7) treatment could be related to this effect exerted by Ang-(1–7). Hemodynamic effects with improved delivery of insulin and glucose to peripheral tissues could also be involved in the beneficial effects induced by Ang-(1–7) in fructose-fed rats. Ang-(1–7) is a vasodilator, in part due to its recently demonstrated capability of activating the endothelial nitric oxide synthase (40) and also because of its proven ability to potentiate the action of bradykinin (26). Gestational diabetes is associated with decreased levels of Ang-(1–7), which coincides with endothelial dysfunction during pregnancy (35). This agrees with the beneficial effects (vasodilation, improvement of glucose, and lipid metabolism) exerted by Ang-(1–7).

Among the serine residues of the IRS-1 that become phosphorylated in response to risk factors for insulin resistance, Ser^{307} has been studied extensively and has become a molecular indicator of insulin resistance (1, 2, 24). Phosphorylation of IRS-1 at this site in skeletal muscle and adipose tissue is increased in insulin-resistant states (11). IRS-1 is phosphorylated at Ser^{307} by multiple kinases, including JNK (1, 24), mTOR (7), and IKK (16). Accordingly, in our current study, we have investigated the phosphorylation of IRS-1 Ser^{307} and shown that fructose-fed rats display an increase in IRS-1 Ser^{307} phosphorylation levels together with increased activation of the serine kinases JNK and mTOR in skeletal muscle and adipose tissue. Moreover, we demonstrated that improvement of insulin signaling associated with Ang-(1–7) treatment is accompanied with decreased phosphorylation at this inhibitory residue and

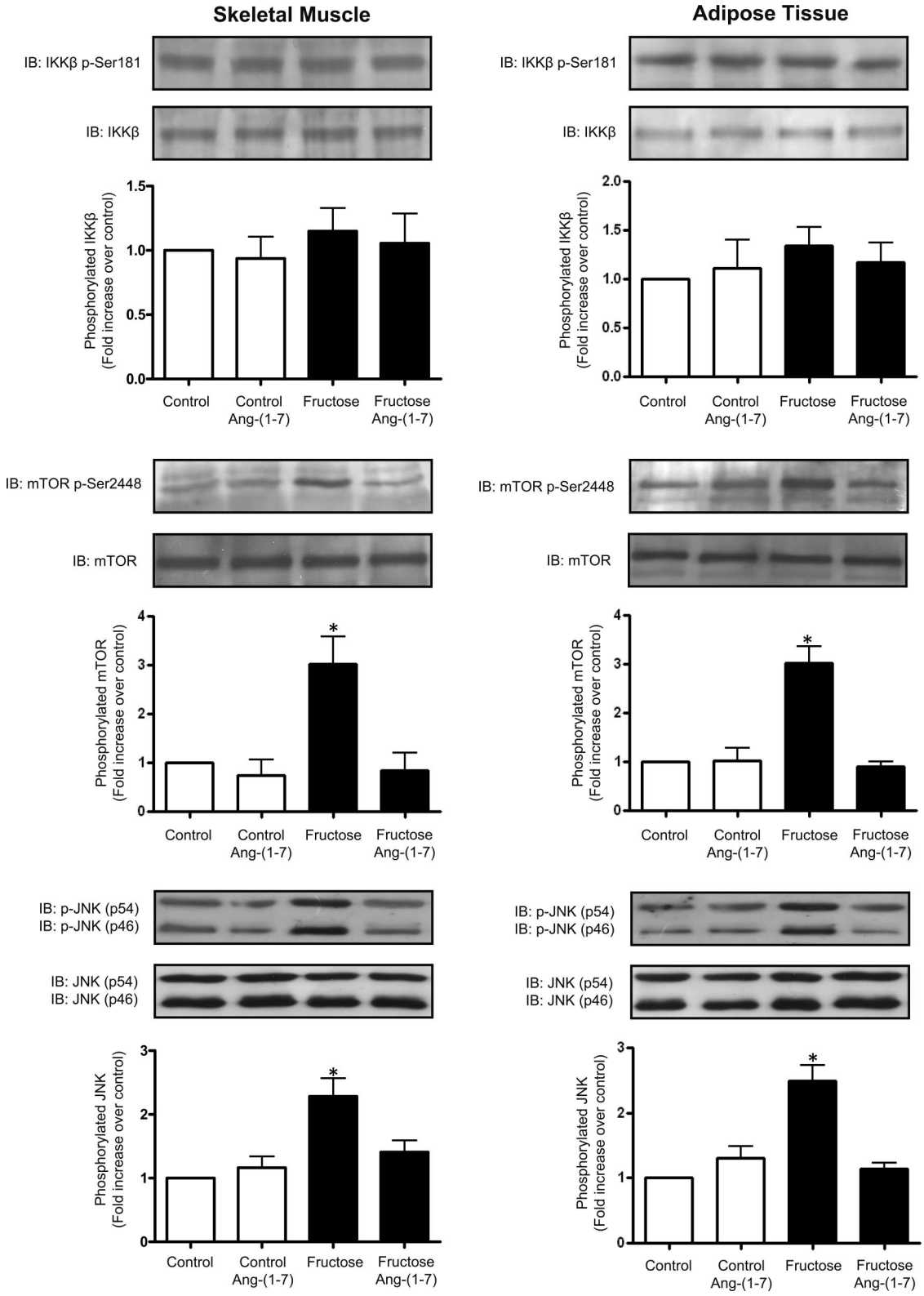

Fig. 7. Phosphorylation and abundance of inhibitor of κB kinase (IKKβ), JNK, and mammalian target of rapamycin (mTOR). Data are from saline-injected rats, as described in the legend to Fig. 1. Phosphorylation of IKKβ, mTOR, JNK or was measured by specific IB. Membranes were reprobed with specific anti-peptide antibody to determine protein abundance. Quantification of phosphorylation by scanning densitometry is given below IB. Scanning data obtained from 6 independent experiments are expressed as fold increase over saline-injected (basal) control phosphorylation ± SE. *$P < 0.05$ vs. insulin-stimulated control values.

decreased activation levels of JNK and mTOR in skeletal muscle and adipose tissue of fructose-fed rats. This finding suggests an additional mechanism by which Ang-(1–7) exerts beneficial effects on the insulin-signaling system.

In conclusion, in the current study we provide novel data suggesting that Ang-(1–7) ameliorates insulin resistance in a model of metabolic syndrome via a mechanism that could involve the modulation of insulin signaling and particularly the modulation of the mTOR pathway involved in phosphorylation of IRS-1 at Ser residue 307. Together with the recently reported phenotype of Mas-knockout receptor mice (43), our current findings reinforce the notion that Ang-(1–7) possesses a role in metabolic processes.

GRANTS

F. P. Dominici, M. M. Gironacci, C. A. Taira, and D. Turyn are Career Investigators from Consejo Nacional de Investigaciones Científicas y Tecnológicas de Argentina (CONICET) and received grant support from the University of Buenos Aires (UBA), CONICET, and Agencia Nacional de Promoción Científica y Tecnológica of Argentina. J. F. Giani is a research fellow from UBA; M. A. Mayer and M. C. Muñoz are research fellows from CONICET.

REFERENCES

1. **Aguirre V, Uchida T, Yenush L, Davis R, White MF.** The c-Jun NH_2-terminal kinase promotes insulin resistance during association with insulin receptor substrate-1 and phosphorylation of Ser^{307}. *J Biol Chem* 275: 9047–9054, 2000.
2. **Aguirre V, Werner ED, Giraud J, Lee YH, Shoelson SE, White MF.** Phosphorylation of Ser307 in insulin receptor substrate-1 blocks interactions with the insulin receptor and inhibits insulin action. *J Biol Chem* 277: 1531–1537, 2002.
3. **Andraws R, Brown DL.** Effect of inhibition of the renin-angiotensin system on development of type 2 diabetes mellitus (meta-analysis of randomized trials). *Am J Cardiol* 99: 1006–1112, 2007.
4. **Benter IF, Yousif MH, Cojocel C, Al-Maghrebi M, Diz DI.** Angiotensin-(1–7) prevents diabetes-induced cardiovascular dysfunction. *Am J Physiol Heart Circ Physiol* 292: H666–H672, 2007.
5. **Benter IF, Yousif MH, Dhaunsi GS, Kaur J, Chappell MC, Diz DI.** Angiotensin-(1–7) prevents activation of NADPH oxidase and renal vascular dysfunction in diabetic hypertensive rats. *Am J Nephrol* 28: 25–33, 2008.
6. **Bezerra RM, Ueno M, Silva MS, Tavares DQ, Carvalho CRO, Saad MJ.** A high fructose diet affects the early steps of insulin action in muscle and liver of rats. *J Nutr* 130: 1531–1535, 2000.
7. **Carlson CJ, White MF, Rondinone CM.** Mammalian target of rapamycin regulates IRS-1 serine 307 phosphorylation. *Biochem Biophys Res Commun* 316: 533–539, 2004.
8. **Carvalho CR, Thirone AC, Gontijo JA, Velloso LA, Saad MJ.** Effect of captopril, losartan, and bradykinin on early steps of insulin action. *Diabetes* 46: 1950–1957, 1997.
9. **Dai S, McNeill JH.** Fructose-induced hypertension in rats is concentration- and duration-dependent. *J Pharmacol Toxicol Methods* 33: 101–107, 1995.
10. **DeFronzo RA.** Insulin resistance: a multifaceted syndrome responsible for NIDDM, obesity, hypertension, dyslipidaemia and atherosclerosis. *Neth J Med* 50: 191–197, 1997.
11. **Draznin B.** Molecular mechanisms of insulin resistance: serine phosphorylation of insulin receptor substrate-1 and increased expression of p85alpha: the two sides of a coin. *Diabetes* 55: 2392–2397, 2006.
12. **Eckel RH, Grundy SM, Zimmet PZ.** The metabolic syndrome. *Lancet* 365: 1415–1428, 2005.
13. **Erlich Y, Rosenthal T.** Effect of angiotensin-converting enzyme inhibitors on fructose induced hypertension and hyperinsulinemia in rats. *Clin Exp Pharmacol Physiol Suppl* 22: S347–S349, 1995.
14. **Ferrario CM, Trask AJ, Jessup JA.** Advances in biochemical and functional roles of angiogtensin-converting enzyme 2 and angiotensin-(1–7) in regulation of cardiovascular function. *Am J Physiol Heart Circ Physiol* 289: H2281–H2290, 2005.
15. **Furuhashi M, Ura N, Takizawa H, Yoshida D, Moniwa N, Murakami H, Higashiura K, Shimamoto K.** Blockade of the renin-angiotensin system decreases adipocyte size with improvement in insulin sensitivity. *J Hypertens* 22: 1977–1982, 2004.
16. **Gao Z, Hwang D, Bataille F, Lefevre M, York D, Quon MJ, Ye J.** Serine phosphorylation of insulin receptor substrate 1 by inhibitor kappa B kinase complex. *J Biol Chem* 277: 48115–48121, 2002.
17. **Giani JF, Gironacci MM, Muñoz MC, Peña C, Turyn D, Dominici FP.** Angiotensin-(1–7) stimulates the phosphorylation of JAK2, IRS-1 and Akt in rat heart in vivo: role of the AT_1 and Mas receptors. *Am J Physiol Heart Circ Physiol* 293: H1154–H1163, 2007.
18. **Grobe JL, Mecca AP, Lingis M, Shenoy V, Bolton TA, Machado JM, Speth RC, Raizada MK, Katovich MJ.** Prevention of angiotensin II-induced cardiac remodeling by angiotensin-(1–7). *Am J Physiol Heart Circ Physiol* 292: H736–H742, 2007.
19. **Grobe JL, Mecca AP, Mao H, Katovich MJ.** Chronic angiotensin-(1–7) prevents cardiac fibrosis in DOCA-salt model of hypertension. *Am J Physiol Heart Circ Physiol* 290: H2417–H2423, 2006.
20. **Grundy SM.** Metabolic syndrome: connecting and reconciling cardiovascular and diabetes worlds. *J Am Coll Cardiol* 47: 1093–1100, 2006.
21. **Henriksen EJ, Jacob S, Kinnick TR, Teachey MK, Krekler M.** Selective angiotensin II receptor antagonism reduces insulin resistance in obese Zucker rats. *Hypertension* 38: 884–890, 2001.
22. **Henriksen EJ.** Improvement of insulin sensitivity by antagonism of the renin-angiotensin system. *Am J Physiol Regul Integr Comp Physiol* 293: R974–R980, 2007.
23. **Higashiura K, Ura N, Takada T, Li Y, Torii T, Togashi N, Takada M, Takizawa H, Shimamoto K.** The effects of an angiotensin-converting enzyme inhibitor and an angiotensin II receptor antagonist on insulin resistance in fructose-fed rats. *Am J Hypertens* 13: 290–297, 2000.
24. **Hirosumi J, Tuncman G, Chang L, Gorgun CZ, Uysal KT, Maeda K, Karin M, Hotamisligil GS.** A central role for JNK in obesity and insulin resistance. *Nature* 420: 333–336, 2002.
25. **Hsie PS.** Reversal of fructose-induced hypertension and insulin resistance by chronic losartan treatment is independent of AT2 receptor activation in rats. *J Hypertens* 23: 2209–2217, 2005.
26. **Iusuf D, Henning RH, van Gilst WH, Roks AJ.** Angiotensin-(1–7): pharmacological properties and pharmacotherapeutic perspectives. *Eur J Pharmacol* 585: 303–312, 2008.
27. **Jandeleit-Dahm KA, Tikellis C, Reid CM, Johnston CI, Cooper ME.** Why blockade of the renin-angiotensin system reduces the incidence of new-onset diabetes. *J Hypertens* 23: 463–473, 2005.
28. **Kamari Y, Harari A, Shaish A, Peleg E, Sharabi Y, Harats D, Grossman E.** Effect of telmisartan, angiotensin II receptor antagonist, on metabolic profile in fructose-induced hypertensive, hyperinsulinemic, hyperlipidemic rats. *Hypertens Res* 31: 135–140, 2008.
29. **Kobayashi R, Nagano M, Nakamura F, Higaki J, Fujioka Y, Ikegami H, Mikami H, Kawaguchi N, Onishi S, Ogihara T.** Role of angiotensin II in high fructose-induced left ventricular hypertrophy in rats. *Hypertension* 21: 1051–1055, 1993.
30. **Liu IM, Tzeng TF, Liou SS, Lan TW.** Myricetin, a naturally occurring flavonol, ameliorates insulin resistance induced by a high-fructose diet in rats. *Life Sci* 81: 1479–1488, 2007.
31. **Matthews DR, Hosker JP, Rudenski AS, Naylor BA, Treacher DF, Turner RC.** Homeostasis model assessment: insulin resistance and beta-cell function from fasting plasma glucose and insulin concentrations in man. *Diabetologia* 28: 412–419, 1985.
32. **Mayer MA, Höcht C, Gironacci M, Opezzo JA, Taira CA, Fernández BE, Puyó AM.** Hypothalamic angiotensinergic-noradrenergic systems interaction in fructose induced hypertension. *Regul Pept* 146: 38–45, 2008.
33. **Muñoz MC, Argentino DP, Dominici FP, Turyn D, Toblli JE.** Irbersartan restores the in vivo insulin signaling pathway leading to Akt activation in obese Zucker rats. *J Hypertens* 24: 1607–1617, 2006.
34. **Nawano M, Anai M, Funaki M, Kobayashi H, Kanda A, Fukushima Y, Inukai K, Ogihara T, Sakoda H, Onishi Y, Kikuchi M, Yazaki Y, Oka Y, Asano T.** Imidapril, an angiotensin-converting enzyme inhibitor, improves insulin sensitivity by enhancing signal transduction via insulin receptor substrate proteins and improving vascular resistance in the Zucker fatty rat. *Metabolism* 48: 1248–1255, 1999.
35. **Nogueira AI, Souza Santos RA, Simões E Silva AC, Cabral AC, Vieira RL, Drumond TC, Machado LJ, Freire CM, Ribeiro-Oliveira A Jr.** The pregnancy-induced increase of plasma angiotensin-(1–7) is blunted in gestational diabetes. *Regul Pept* 141: 55–60, 2007.
36. **Okada K, Hirano T, Ran J, Adachi M.** Olmesartan medoxomil, an angiotensin II receptor blocker ameliorates insulin resistance and de-

creases triglyceride production in fructose-fed rats. *Hypertens Res* 27: 293–299, 2004.
37. **Perkins JM, Davis SN.** The renin-angiotensin aldosterone system: a pivotal role in insulin sensitivity and glycemic control. *Curr Opin Endocrinol Diabetes Obes* 15: 147–152, 2008.
38. **Rao RH.** Effects of angiotensin II on insulin sensitivity and fasting glucose metabolism in rats. *Am J Hypertens* 7: 655–660, 1994.
39. **Richey JM, Ader M, Moore D, Bergman RN.** Angiotensin II induces insulin resistance independent of changes in interstitial insulin. *Am J Physiol Endocrinol Metab* 277: E920–E926, 1999.
40. **Sampaio WO, Souza dos Santos RA, Faria-Silva R, da Mata Machado LT, Schiffrin EL, Touyz RM.** Angiotensin-(1–7) through receptor Mas mediates endothelial nitric oxide synthase activation via Akt-dependent pathways. *Hypertension* 49: 185–192, 2007.
41. **Sánchez-Lozada LG, Tapia E, Jiménez A, Bautista P, Cristóbal M, Nepomuceno T, Soto V, Avila-Casado C, Nakagawa T, Johnson RJ, Herrera-Acosta J, Franco M.** Fructose-induced metabolic syndrome is associated with glomerular hypertension and renal microvascular damage in rats. *Am J Physiol Renal Physiol* 292: F423–F429, 2007.
42. **Santos RA, Ferreira AJ, Simões E Silva AC.** Recent advances in the angiotensin-converting enzyme 2-angiotensin(1–7)-Mas axis. *Exp Physiol* 293: 519–527, 2008.
43. **Santos SH, Fernandes LR, Mario EG, Ferreira AV, Pôrto LC, Alvarez-Leite JI, Botion LM, Bader M, Alenina N, Santos RA.** Mas deficiency in FVB/N mice produces marked changes in lipid and glycemic metabolism. *Diabetes* 57: 340–347, 2008.
44. **Sarzani R, Salvi F, Dessμ-Fulgheri P, Rappelli A.** Renin-angiotensin system, natriuretic peptides, obesity, metabolic syndrome, and hypertension: an integrated view in humans. *J Hypertens* 26: 831–843, 2008.
45. **Shiuchi T, Iwai M, Li HS, Wu L, Min LJ, Li JM, Okumura M, Cui TX, Horiuchi M.** Angiotensin II type-1 receptor blocker valsartan enhances insulin sensitivity in skeletal muscles of diabetic mice. *Hypertension* 43: 1003–1010, 2004.
46. **Sowers JR.** Insulin resistance and hypertension. *Am J Physiol Heart Circ Physiol* 286: H1597–H1602, 2004.
47. **Velloso LA, Folli F, Perego L, Saad MJ.** The multi-faceted cross-talk between the insulin and angiotensin II signaling systems. *Diabetes Metab Res Rev* 22: 98–107, 2006.